

Identification-based 3 DOF model of unmanned surface vehicle using support vector machines enhanced by cuckoo search algorithm

Peng-Fei Xu ^{*}, Chen Cheng, Hong-Xia Cheng, Ya-Lin Shen, Yan-Xu Ding

Institute of Marine Vehicle and Underwater Technology, College of Harbor, Coastal and Offshore Engineering, Hohai University, China

ARTICLE INFO

Keywords:

Unmanned surface vehicle
System identification
Support vector machine
Cuckoo search algorithm
Zigzag test

ABSTRACT

The combination of least square support vector machine (LS-SVM) and cuckoo search (CS) algorithm was first proposed to identify the dynamic models of unmanned surface vehicle (USV). The 3-DOF of Abkowitz model was selected to describe the USV's dynamics. The zigzag test was carried out in the Qinghuai river. The input data and output data obtained by the experiment were selected and filtered to identify the USV's dynamics. The back propagation neural network (BPNN) is a popular method to identify the ship dynamics and was adopted, in this paper, to compare the LSSVM. In addition, the frequently optimization algorithm including particle swarm optimization (PSO) and cross validation (CV) were also selected to enhance the LSSVM which compare to the CS-LSSVM. The results showed that the CS-LSSVM had a better predictive capability than the BPNN, PSO-LSSVM and CV-LSSVM in predicting the surge velocity and sway velocity and the values were close to the experimental data. The related mean square errors of CS-LSSVM was the lowest in these methods and has the fastest convergence speed. It can be tested that CS-LSSVM would be a potential method to online parameter identification for USV in the future.

1. Introduction

With the development of unmanned surface vehicles (USV) have become powerful tools in the military and civil fields such as environmental monitoring, resource exploration and shipping etc. The accuracy dynamic models of an USV is the most significant factor to guarantee that has a good performance in the water. [Zwierzewicz \(2013\)](#) linearized the nonlinear ship model of Norrbin type and utilized the adaptive control method to identify the course-keeping control system. [Sonnenburg and Woolsey \(2013\)](#) adopted the first order linear Nomoto model with the linear sideslip model and simplified speed model to track the USV's trajectories. In this paper, the Abkowitz model was utilized to represent the planar dynamics of USV.

When the suitable of dynamic models had been selected, the system identification of the USV's dynamic model was a part of the accreditation process. Towing-tank experiments, captive model experiments ([Sketne et al., 2004](#)), computational fluid dynamics (CFD) and system identification. Among these approaches, the system identification combined with full-scale and free-running model is becoming an

effective method to construct the system's dynamic model. The method of system identification is to describe a model that best represent the input-output data relationships.

The system identification has been rapidly in the ship's controllability such as the maximum likelihood method ([Aström et al, 1979](#)), the Kalman filter method ([Yoon and Rhee, 2003](#)), the recursive least square method ([Nguyen, 2008](#)), the least square method ([Xu et al., 2014](#)). During the recent year, the modern artificial intelligent technology has been utilized to identify the ship's dynamical models. [Rajesh and Bhattacharyya \(2008\)](#) utilized artificial neural network method to deal with the system identification of the large tanker. The Levenberg-Marquardt algorithm was utilized to train the net, and different numbers of the hidden neurons were compared to select the best choice for construction of the neural network. [Pan et al. \(2013\)](#) utilized an efficient neural network (NN) approach to track the motion of the autonomous surface vehicle with unknown ship dynamic. [Shin et al. \(2017\)](#) demonstrated the particle swarm optimization (PSO) with an adaptive control algorithm to predict the trajectory of the unmanned surface vehicle. Support vector machines method (SVM), which has a

* Corresponding author. Institute of Marine Equipment and Underwater Technology, College of Harbor, Coastal and Offshore Engineering, Hohai University, Nanjing, Jiangsu Province, 210000, China..

E-mail address: xupengfei@hhu.edu.cn (P.-F. Xu).

URL: <http://ghxy.hhu.edu.cn/2016/0114/c10224a105843/page.htm> (P.-F. Xu).

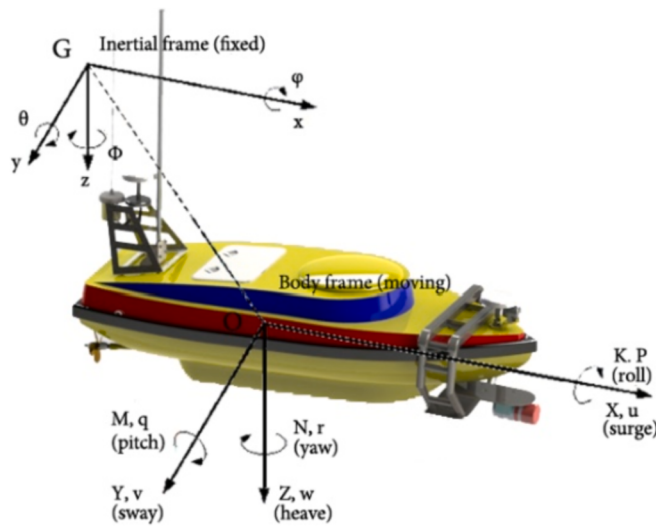


Fig. 1. Reference frames for unmanned surface vehicle.

Table 1
Principal parameters of the USV.

Parameters	Values
Length	1.8m
Breadth	0.7m
Block coefficient	0.47
Mass	70 kg
Height	0.48m
Aspect ratio	1.489
Propeller diameter	0.14m

well promotion ability, becomes more attractive in the system identification. Luo and Zou (2009) applied SVM to identify the hydrodynamic derivatives of Abkowitz model from the simulated free-running model test results and then used the regressive Abkowitz model to represent zigzag tests. The results showed that the regressive model has a good generalization performance. Xu et al. (2013) proposed the LSSVM method to construct the nonlinear dynamic models of the underwater vehicle. The identification results were also show good fitness.

In this paper, the main contributions can be concluded as follow: First, the Abkowitz model was discretized to represent the 3 DOF of USV which can more easily calculate the hydrodynamic parameters; furthermore, to date, the SVM method enhanced by the Cuckoo search algorithm is proposed and that is the first time to identify the dynamic models of USV in three degrees of freedom (3-DOF). This method made further effort to improve the application of SVM in marine field and obtain the solution of optimizing structural parameters in SVM. The results showed that the method proposed in this paper is better than

other mainstream approaches which has been considered in open literatures.

The structure of this paper can be viewed as follow. Section 2 describes the Abkowitz model to represent the dynamics of the USV. Taylor's formula is utilized to expand the term of forces. Section 3 depicts the formulation of the LS-SVM and CS algorithm, the input samples and output samples are determined by discretizing equations. In section 4, the experiment is carried out in the Qinghuai river and the data is obtained which is utilized to identify the USV's dynamics. Finally, concluding remarks are summarized in Section 5.

2. Dynamic model of ships

Generally, ships moving in six degrees of freedom. The two reference frames, a body-fixed frame and an earth-fixed frame, are always utilized to describe the motion of the ship (Fossen, 2011) and it can be viewed in Fig. 1. The notations of six freedom are surge, sway, heave, roll, yaw and pitch which was enacted by SNAME. In order to simply describe the motion of the USV, the three degrees of freedom (surge, sway and yaw) in the horizontal planar motion are considered in this paper. In addition, the USV in this research is designated as Deepsea Warriors uBoat (DW-uBoat) which is designed independently by institute of marine equipment and underwater technology in Hohai university. The principal parameters of USV are shown in Table 1.

Ship maneuvering motion equation can be established based on Newton's second law (Zhang and Zou, 2011):

$$\begin{cases} (m - X_u)\dot{u} = f_1(u, v, r, \delta) \\ (m - Y_v)\dot{v} + (mx_G - Y_r)\dot{r} = f_2(u, v, r, \delta) \\ (mx_G - N_v)\dot{v} + (I_z - N_r)\dot{r} = f_3(u, v, r, \delta) \end{cases} \quad (1)$$

where u denotes the longitudinal velocity component, v the transverse velocity component, r the heading rate around the z -axis, δ the rudder angle, m the mass of the ship, I_z the moment of inertia, x_G the center of ship's gravity, X_u, Y_v, Y_r, N_v, N_r the hydrodynamic derivatives.

However, the USV proposed in this paper dose not have the rudder, the propulsion system of the DW-uboat is differential thruster type. The equivalent rudder angle can be expressed by revolution speed of left and right propellers (Wei et al., 2015):

$$\delta = \frac{1}{2}K_N k_N \left(\frac{n_N}{U}\right)^2 \left(i_{(s)} \left(\frac{y_G}{x_G} \left(1 - \frac{\varphi_{(s)}^2}{2} \right) + \varphi_{(s)} \right) + i_{(p)} \left(-\frac{y_G}{x_G} \left(1 - \frac{\varphi_{(p)}^2}{2} \right) + \varphi_{(p)} \right) \right) \quad (2)$$

where: K_N denotes the scale coefficient, k_N the reference thrust coefficient, n_N the reference revolution, $i_{(s)}$ and $i_{(p)}$ the thrust ratio of left and right propellers to reference thrust, x_G and y_G the horizontal length between the gravity point and left/right propellers.

According to the Eq. (1), the nondimensional Abkowitz model can be written as:

$$\begin{bmatrix} m' - X'_u & 0 & 0 \\ 0 & m' - Y'_v & m' \dot{x}'_G - Y'_r \\ 0 & m' \dot{x}'_G - N'_v & I'_z - N'_r \end{bmatrix} \begin{bmatrix} \Delta \dot{u}' \\ \Delta \dot{v}' \\ \Delta \dot{r}' \end{bmatrix} = \begin{bmatrix} \Delta f'_1 \\ \Delta f'_2 \\ \Delta f'_3 \end{bmatrix} \quad (3)$$

where:

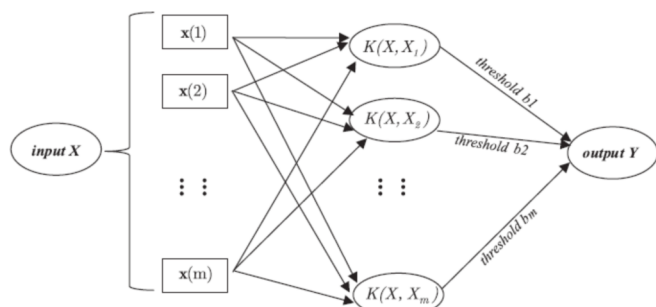


Fig. 2. System structure diagram of SVM.

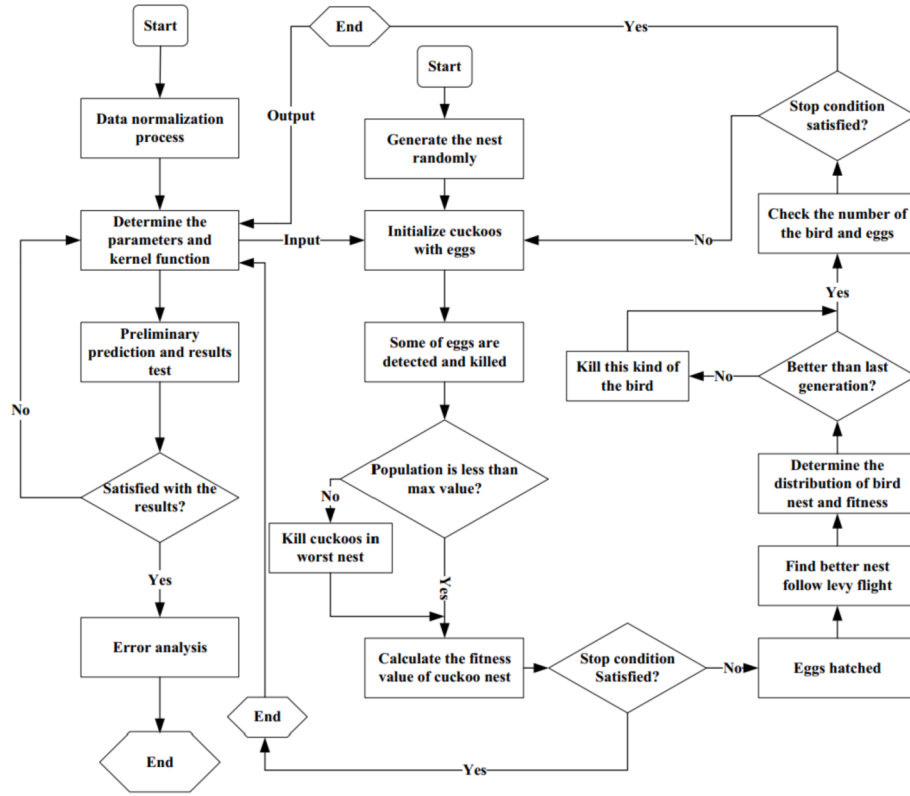


Fig. 3. The flowchart of CS-LSSVM.

$$\begin{aligned}
m' &= \frac{m}{\frac{1}{2}\rho L^3}, \quad x'_G = \frac{x_G}{L}, \quad I'_z = \frac{I_z}{\frac{1}{2}\rho L^5}, \\
\Delta u' &= \frac{\Delta u}{V}, \quad \Delta v' = \frac{\Delta v}{V}, \quad \Delta r' = \frac{L\Delta r}{V}, \\
\Delta \delta' &= \Delta \delta, \quad \Delta \dot{u} = \frac{\Delta \dot{u}}{\left(\frac{V^2}{L}\right)}, \quad \Delta \dot{v} = \frac{\Delta \dot{v}}{\left(\frac{V^2}{L}\right)}, \\
\Delta \dot{r} &= \frac{\Delta \dot{r}}{\left(\frac{V^2}{L}\right)}, \quad X'_u = \frac{X_u}{\frac{1}{2}\rho L^3}, \quad Y'_v = \frac{Y_v}{\frac{1}{2}\rho L^3}, \\
Y'_r &= \frac{Y_r}{\frac{1}{2}\rho L^4}, \quad N'_v = \frac{N_v}{\frac{1}{2}\rho L^4}, \quad N'_r = \frac{N_r}{\frac{1}{2}\rho L^5} \\
\Delta f'_1 &= X'_u \Delta u' + X'_{uu} \Delta u'^2 + X'_{uuu} \Delta u'^3 + X'_{vv} \Delta v'^2 + X'_{rr} \Delta r'^2 + X'_{vr} \Delta v' \Delta r' + X'_{\delta\delta} \Delta \delta'^2 \\
&+ X'_{\delta\delta u} \Delta \delta'^2 \Delta u' + X'_{v\delta} \Delta v' \Delta \delta' + X'_{v\delta u} \Delta v' \Delta \delta' \Delta u' \\
\Delta f'_2 &= Y'_v \Delta v' + Y'_r \Delta r' + Y'_{vv} \Delta v'^3 + Y'_{vvr} \Delta v'^2 \Delta r' + Y'_{vu} \Delta v' \Delta u' + Y'_{ru} \Delta r' \Delta u' + Y'_{\delta} \Delta \delta' + Y'_{\delta\delta\delta} \Delta \delta'^3 \\
&+ Y'_{\delta u} \Delta \delta' \Delta u' + Y'_{\delta uu} \Delta \delta' \Delta u'^2 + Y'_{v\delta\delta} \Delta v' \Delta \delta'^2 + Y'_{v\delta\delta} \Delta v'^2 \Delta \delta' + Y_0 + Y'_{0u} \Delta u' + Y'_{0uu} \Delta u'^2 \\
\Delta f'_3 &= N'_v \Delta v' + N'_r \Delta r' + N'_{vv} \Delta v'^3 + N'_{vvr} \Delta v'^2 \Delta r' + N'_{vu} \Delta v' \Delta u' + N'_{ru} \Delta r' \Delta u' + N'_{\delta} \Delta \delta' + N'_{\delta\delta\delta} \Delta \delta'^3 \\
&+ N'_{\delta u} \Delta \delta' \Delta u' + N'_{\delta uu} \Delta \delta' \Delta u'^2 + N'_{v\delta\delta} \Delta v' \Delta \delta'^2 + N'_{v\delta\delta} \Delta v'^2 \Delta \delta' + N_0 + N'_{0u} \Delta u' + N'_{0uu} \Delta u'^2
\end{aligned} \tag{4}$$

where u denotes the longitudinal velocity component, v the transverse velocity component, r the heading rate around the z -axis, δ the rudder angle, m the mass of the ship, I_z the moment of inertia, x_G the center of ship's gravity, X_u, Y_v, Y_r, N_v, N_r the hydrodynamic derivatives, ρ the mass density of fluid, L the length of the ship, V the ship forward speed, L the length of USV.

3. Parameter identification using SVM enhanced by CS

3.1. SVM formulation

Support vector machines (SVM), a novel method of modern artificial intelligence technology, was proposed in 1990s (Vapnik, 2000). SVM is a statistical learning method based on VC dimension theory and structural risk minimization principle. It has a good promotion ability to handle the classification issues and regression issues. The procedure of the SVM can be viewed in Fig. 2. K is kernel function which has ability of transforming the input series X to another space (Roodposhti et al., 2017). The classification (regression) function of high dimension space

$$\Delta f'_2 = Y'_v \Delta v' + Y'_r \Delta r' + Y'_{vv} \Delta v'^3 + Y'_{vvr} \Delta v'^2 \Delta r' + Y'_{vu} \Delta v' \Delta u' + Y'_{ru} \Delta r' \Delta u' + Y'_{\delta} \Delta \delta' + Y'_{\delta\delta\delta} \Delta \delta'^3 \tag{6}$$

$$\Delta f'_3 = N'_v \Delta v' + N'_r \Delta r' + N'_{vv} \Delta v'^3 + N'_{vvr} \Delta v'^2 \Delta r' + N'_{vu} \Delta v' \Delta u' + N'_{ru} \Delta r' \Delta u' + N'_{\delta} \Delta \delta' + N'_{\delta\delta\delta} \Delta \delta'^3 \\
+ N'_{\delta u} \Delta \delta' \Delta u' + N'_{\delta uu} \Delta \delta' \Delta u'^2 + N'_{v\delta\delta} \Delta v' \Delta \delta'^2 + N'_{v\delta\delta} \Delta v'^2 \Delta \delta' + N_0 + N'_{0u} \Delta u' + N'_{0uu} \Delta u'^2 \tag{7}$$



Fig. 4. DW-uboot voyages in Qing-huai river.

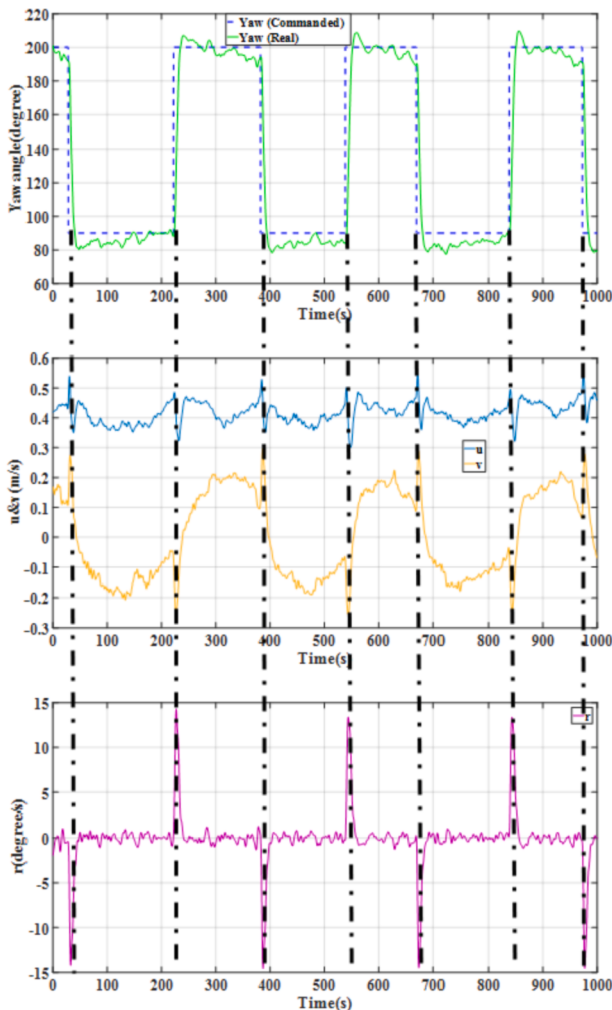


Fig. 5. The data from part of the USV trajectory.

can be achieved via selecting the appropriate kernel function. Then the structure of SVM can be obtained by training input data and output data.

SVM method includes ϵ -SVM, ν -SVM and least square-SVM (LSSVM), etc. Suykens and Vandewalle (1999) proposed that the LSSVM was able to synchronously decrease estimation error in the input – output data (the empirical risk) and the model complexity (the structural risk) for regression issues and classification issues. The equation can be viewed as follow:

$$y(x) = \omega^T \varepsilon(x) + b \quad (x \in R^n, y \in R) \quad (8)$$

where x denotes the input data, y the output data, ω the matrix of weights, $\varepsilon(\cdot)$ the mapping to a high-dimensional Hilbert space and b the bias. The training set was utilized to optimize weight space ω :

$$\min_{\omega, b, e} J(\omega, e) = \frac{1}{2} \omega^T \omega + C \sum_{i=1}^{N_s} e_i^2 \quad (9)$$

Table 2
Identified parameters by CS-LSSVM.

A	CS-SVM	B	CS-SVM	C	CS-SVM
a_1	-0.002	b_1	0.00237	c_1	-0.00517
a_2	0.000128	b_2	0.00211	c_2	0.000849
a_3	-0.00005	b_3	0.001508	c_3	-3.62E-05
a_4	0.000121	b_4	-5.42E-05	c_4	-0.00259
a_5	0.0992	b_5	0.006043	c_5	-0.00259
a_6	-0.4501	b_6	0.006043	c_6	1.521236
a_7	0.0057	b_7	-1.33421	c_7	-2.73E-07
a_8	-0.0029	b_8	1.61E-06	c_8	0.423456
a_9	0.423	b_9	-0.0831	c_9	1.30E-05
a_{10}	0.423	b_{10}	-0.00031	c_{10}	0.000105
		b_{11}	-0.00184	c_{11}	0.003286
		b_{12}	-8.53E-05	c_{12}	0.003142
		b_{13}	-0.00015	c_{13}	0.000205
		b_{14}	-0.00015	c_{14}	0.000205
		b_{15}	-0.00038	c_{15}	0.000777

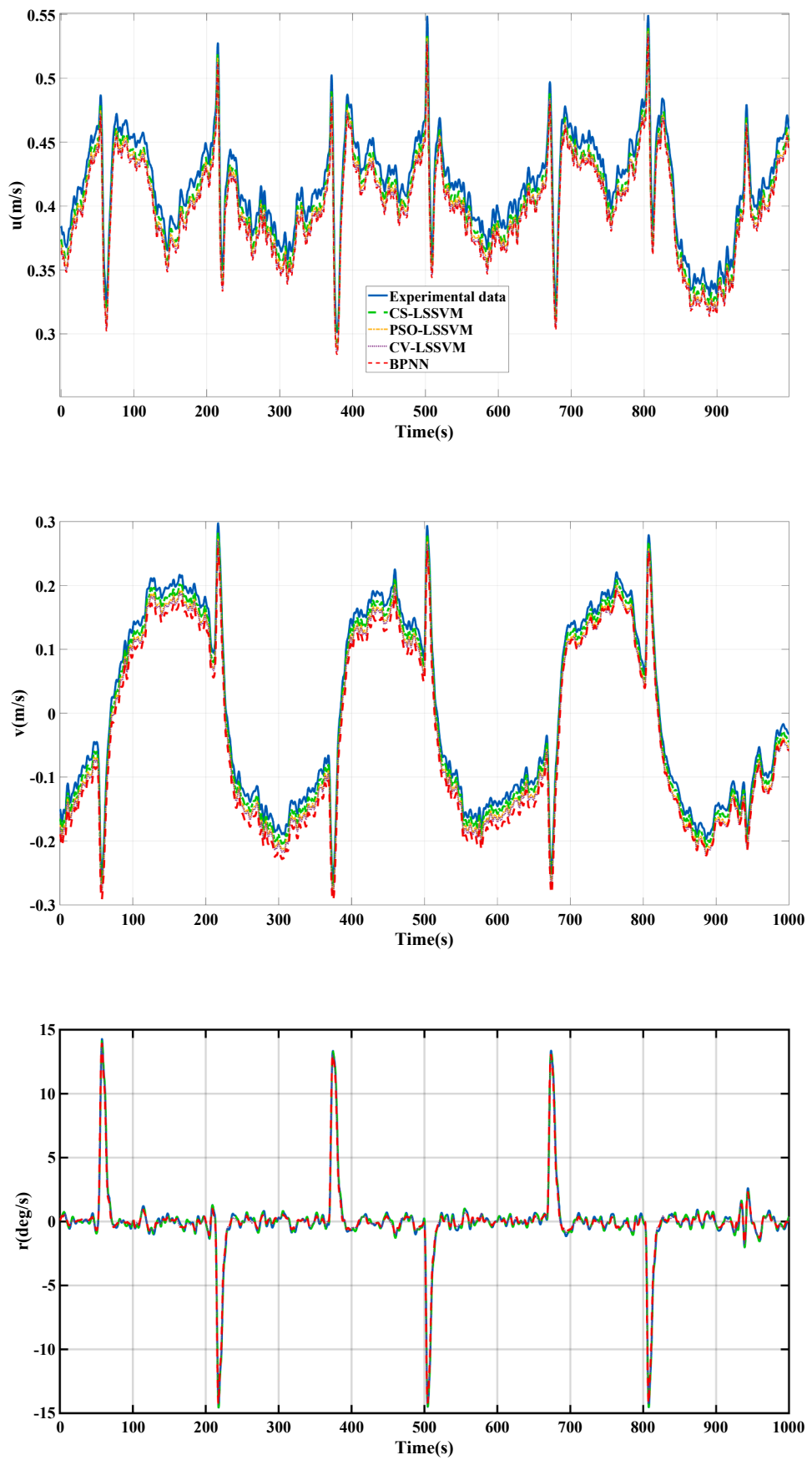


Fig. 6. Comparisons of the surge velocity, sway velocity and yaw rate predicted by these methods in training trajectory.

Table 3

The Comparison of MSE among these methods in training trajectory.

		CS-LSSVM	PSO-LSSVM	CV-LSSVM	BPNN
Surge velocity	MSE	0.0018	0.0023	0.0025	0.0077
	TIME	34s	45s	53s	66s
Sway velocity	MSE	0.0021	0.0028	0.0029	0.0056
	TIME	41s	47s	49s	58s
Yaw rate	MSE	0.0008	0.0009	0.0009	0.0013
	TIME	33s	36s	41s	52s

subject to

$$y_i = \omega^T \varepsilon(x_i) + b + e_i \quad (10)$$

where $e_i (i = 1, \dots, N_s)$ denote the regression error, C the regularization parameter, N_s the number of samples. Owing to the weight space becoming the infinite dimension, the Lagrange multipliers are selected to solve the problem in the primal weight space.

$$J(\omega, b, e, \alpha) = J(\omega, e) - \sum_{i=1}^{N_s} \alpha_i (\omega^T \varepsilon(x_i) + b + e_i - y_i) \quad (11)$$

where $\alpha_i (i = 1, 2, \dots, N)$ denotes the Lagrange multipliers, then the derivatives of ω, b, e_i, α_i are computed and set to be zero which can be expressed as follow:

$$\left\{ \begin{array}{l} \frac{\partial J(\omega, b, e, \alpha)}{\partial \omega} = 0 \rightarrow \omega = \sum_{i=1}^{N_s} \alpha_i \varepsilon(x_i) \\ \frac{\partial J(\omega, b, e, \alpha)}{\partial b} = 0 \rightarrow \sum_{i=1}^{N_s} \alpha_i = 0 \\ \frac{\partial J(\omega, b, e, \alpha)}{\partial e_i} = 0 \rightarrow \alpha_i = C e_i \\ \frac{\partial J(\omega, b, e, \alpha)}{\partial \alpha_i} = 0 \rightarrow \omega^T \varepsilon(x_i) + b + e_i - y_i = 0 \end{array} \right. \quad (12)$$

The kernel function is also utilized to work in large dimensional feature spaces without complicated calculations on them. The function yields as follow:

$$y(x) = \sum_{i=1}^{N_s} \alpha_i K(x, x_i) + b \quad (13)$$

where $K(x, x_i)$ is kernel function and Eq. (14) can be used to obtain the regression model. The types of the kernel function are varied and the linear kernel is adopted to solve the problem of the parametric identification. Since the identification equations of dynamic models are linear with respect to identification parameters (Zhu et al., 2017).

$$K(x_i, x_j) = \langle x_i, x_j \rangle \quad (14)$$

3.2. Cuckoo search (CS) algorithm

CS is a swarm intelligence and smart optimization algorithm which was developed by the Xin-she Yang of Cambridge University and Suash Deb of C. V. Raman Engineering Institute in 2009 (Nadjemi et al., 2017). The characteristics of CS algorithm include the parasitic reproduction strategy of the cuckoo population and levy flight behavior (Rakhshani et al., 2016). The cuckoo never brings up eggs in its own nest, they will search in an area to find a best bird nest to left its eggs randomly. If parasitic eggs were found by other birds, the cuckoo would give up this area the next time. The path and position of cuckoo's nest can be demonstrated as follows:

$$x_i^{t+1} = x_i^t + \alpha \oplus L(\mu, v), \quad i = 1, 2, \dots, N \quad (15)$$

where x_i^t denotes the position of the i -th bird's nest in the t -th iteration;

α the factor of the step size to control the random walk step; $L(\mu, v)$ the random path of step size. The Mantegna algorithm is utilized to represent levy flight and step size can be calculated as:

$$L(\mu, v) = \frac{\mu}{|v|^{1/\beta}} \quad (16)$$

$$\begin{cases} \mu \sim N(0, \sigma_\mu^2) \\ v \sim N(0, \sigma_v^2) \end{cases} \quad (17)$$

$$\sigma_\mu = \left(\frac{\Gamma(1+\beta)\sin\pi\beta/2}{\Gamma[(1+\beta)/2]2^{(\beta-1)/2}\beta} \right)^{1/\beta} \quad (18)$$

$$\sigma_v = 1 \quad (19)$$

where β was set to 1.5 in order to make full use of the information provided by the current optimal individual (Wang et al., 2019). The random number r is generated which belongs to zero and one. If the random number is greater than the probability of discovery, the value of the x_i^t will be updated. In CS algorithm, the step generated by levy flight is random and lack of adaptability which can not guarantee the converge speed of the results. Therefore, the step size can be adjusted by the following method (Walton et al., 2013):

$$step_i = step_{\min} + (step_{\max} - step_{\min})d_i \quad (20)$$

$$d_i = \frac{\|n_i - n_{best}\|}{d_{\max}} \quad (21)$$

where $step_{\max}$ and $step_{\min}$ denote the largest step size and least step size. n_i the position of the i -th bird's nest; n_{best} the best status of bird's nest; d_{\max} the maximum distance between the best position of the bird's nest and other nests.

3.3. Regularization parameter selection based on CS

The regularization parameter is a vital parameter to ensure that the SVM have a perfect performance in parametric identification. CS is proposed that is an effective optimization algorithm to converge the global optimal value and obtain the regularization parameter.

The CS algorithm is utilized to optimize the parameter C of SVM, the flow chart can be viewed as Fig. 3 and the procedures can be demonstrated as follow:

- (1) Set the initial range of the penalty parameter C , the coefficient of kernel function σ , the maximum step size $step_{\max}$, the minimum step size $step_{\min}$ and the maximum numbers of iteration M_{\max} by experience.
- (2) The probability of the nest being found P_a are set to 0.75 which can randomly generate the n bird's nests $n_i^{(0)}$. Every nest represents the individual penalty parameter and coefficient of kernel function, the error of the fold of k-fold cross validation v is calculated and the best current location of bird's nest $x_b^{(0)}$ with related error is found.
- (3) Calculate step size of the levy flight by Eq. (21) and Eq. (22) to update the other location of the bird's nest. A new nest is generated and the related error is obtained.
- (4) Compare the predicted error in the new location of bird's nest p_t and last location of bird's nest p_{t-1} and choose the better location of the bird's nest k_t .
- (5) The probability of the nest being found P_a is compared to the random number r . Nests with less probability of being found will be contained, and nests with bigger probability of being found in p_t needs to be regenerated. Calculate the fitness of new nest and compared it with that of the nests in p_t . Then a better position will

- replace the worse location which cause a group of gorgeous location of bird's nest p_t .
- (6) The optimal bird's nest will be obtained in step (5), if the fitness meets the requirement of the end condition, stop searching and exporting the global best fitness and the best location of nest. If not, back to the step (3) to iteration.

3.4. Construction of samples for identification

In the state of straight forward motion with constant speed, we have:

$$\begin{cases} u_0 = V, v_0 = r_0 = \delta_0 = 0 \\ u = u_0 + \Delta u, v = \Delta v, r = \Delta r, \delta = \Delta \delta \\ \dot{u} = \Delta \dot{u}, \dot{v} = \Delta \dot{v}, \dot{r} = \Delta \dot{r} \end{cases} \quad (22)$$

Then:

$$U = \sqrt{(u_0 + \Delta u)^2 + \Delta v^2} \quad (23)$$

U is resultant speed in the horizontal plane, $\Delta u, \Delta v, \Delta r, \Delta \delta, \Delta \dot{u}, \Delta \dot{v}, \Delta \dot{r}$ are disturbing quantity of speed (angular speed), rudder angle and acceleration (angular acceleration).

Eq. (4) can be transformed into the following state space equation:

$$\begin{cases} \Delta \dot{u} = \frac{\Delta f'_1}{m' - X'_u} \\ \Delta \dot{v} = \frac{(I'_z - N'_r) \Delta f'_2 - (m' x'_G - Y'_r) \Delta f'_3}{T} \\ \Delta \dot{r} = \frac{(m' - Y'_v) \Delta f'_3 - (m' x'_G - N'_v) \Delta f'_2}{T} \end{cases} \quad (24)$$

where

$$T = (I'_z - N'_r)(m' - Y'_v) - (m' x'_G - Y'_r)(m' x'_G - N'_v) \quad (25)$$

Euler's stepping method was utilized to discretize the Eq. (25) as follow:

$$\begin{cases} \dot{u}(k) = \frac{[u(k+1) - u(k)]}{h} \\ \dot{v}(k) = \frac{[v(k+1) - v(k)]}{h} \\ \dot{r}(k) = \frac{[r(k+1) - r(k)]}{h} \end{cases} \quad (26)$$

According to the Eq. (4) and Eq. (12), the discretizing equation can be viewed as follow:

$$\begin{aligned} \Delta u(k+1) &= \Delta u(k) \\ &+ \frac{h}{L(m' - X'_u)} \left[X'_{uu} \Delta u(k) U(k) + X'_{uuu} \Delta u^2(k) + \frac{X'_{uuu} \Delta u^3(k)}{U(k)} \right. \\ &\quad + X'_{vv} \Delta v^2(k) + X'_{rr} \Delta r^2(k) L^2 + X'_{\delta\delta} \Delta \delta^2(k) U^2(k) \\ &\quad + X'_{\delta\delta u} \Delta \delta^2(k) \Delta u(k) U(k) + X'_{vr} \Delta v(k) \Delta r(k) L \\ &\quad \left. + X'_{v\delta} \Delta v(k) \Delta \delta(k) U(k) + X'_{v\delta u} \Delta v(k) \Delta \delta(k) \Delta u(k) \right] \end{aligned} \quad (27)$$

$$\begin{aligned} \Delta v(k+1) &= \Delta v(k) + \frac{h(I'_z - N'_r)}{TL} \\ &+ \frac{h(I'_z - N'_r)}{TL} \left[Y'_0 U^2(k) + Y'_{0u} \Delta u(k) U(k) + Y'_{0uu} \Delta u^2(k) \right. \\ &\quad + Y'_v \Delta v(k) U(k) + Y'_r \Delta r(k) U(k) L \\ &\quad + Y'_\delta \Delta \delta(k) U^2(k) + \frac{Y'_{vvv} \Delta v^3(k)}{U(k)} \\ &\quad + Y'_{\delta\delta\delta} \Delta \delta^3(k) U^2(k) + \frac{Y'_{vvr} \Delta v^2(k) \Delta r(k) L}{U(k)} \\ &\quad + Y'_{vv\delta} \Delta v^2(k) \Delta \delta(k) + Y'_{v\delta\delta} \Delta v(k) \Delta \delta^2(k) U(k) \\ &\quad + Y'_{\delta u} \Delta \delta(k) \Delta u(k) U(k) + Y'_{vu} \Delta v(k) \Delta u(k) \\ &\quad \left. + Y'_{ru} \Delta r(k) \Delta u(k) L + Y'_{\delta uu} \Delta \delta(k) \Delta u^2(k) \right] \\ &N'_o U^2(k) + N'_{0u} \Delta u(k) U(k) + N'_{0uu} \Delta u^2(k) + N'_{v} \Delta v(k) U(k) + \\ &N'_r \Delta r(k) U(k) L + N'_\delta \Delta \delta(k) U^2(k) + \frac{N'_{vvv} \Delta v^3(k)}{U(k)} + \\ &-\frac{h(m' x'_G - Y'_r)}{TL} \left[N'_{\delta\delta\delta} \Delta \delta^3(k) U^2(k) + \frac{N'_{vvr} \Delta v^2(k) \Delta r(k) L}{U(k)} + N'_{vv\delta} \Delta v^2(k) \Delta \delta(k) \right. \\ &\quad + N'_{v\delta\delta} \Delta v(k) \Delta \delta^2(k) U(k) + N'_{\delta u} \Delta \delta(k) \Delta u(k) U(k) \\ &\quad \left. + N'_{vu} \Delta v(k) \Delta u(k) L + N'_{ru} \Delta r(k) \Delta u(k) + N'_{\delta uu} \Delta \delta(k) \Delta u^2(k) \right] \end{aligned} \quad (28)$$

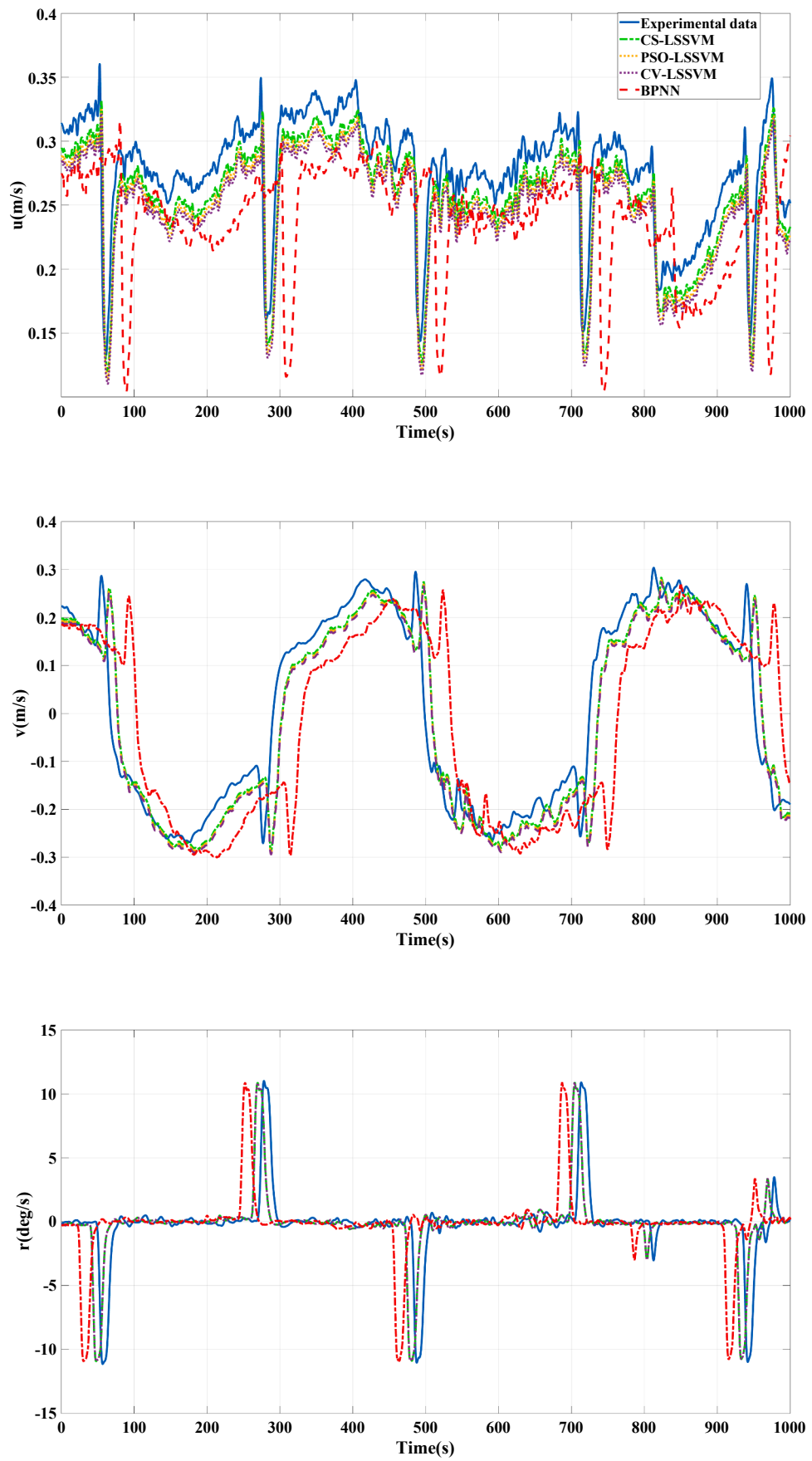


Fig. 7. Comparisons of the surge velocity, sway velocity and yaw rate predicted by these methods in testing trajectory.

$$\Delta r(k+1) = \Delta r(k) - \frac{h(m'x'_G - N'v)}{TL^2} + \left[\begin{array}{l} Y'_0 U^2(k) + Y'_{0u} \Delta u(k) U(k) + Y'_{0uu} \Delta u^2(k) \\ + Y'_v \Delta v(k) U(k) + Y'_r \Delta r(k) U(k) L \\ + Y'_\delta \Delta \delta(k) U^2(k) + \frac{Y'_{vvv} \Delta v^3(k)}{U(k)} \\ + Y'_{\delta\delta\delta} \Delta \delta^3(k) U^2(k) + \frac{Y'_{vvr} \Delta v^2(k) \Delta r(k) L}{U(k)} \\ + Y'_{vv\delta} \Delta v^2(k) \Delta \delta(k) + Y'_{v\delta\delta} \Delta v(k) \Delta \delta^2(k) U(k) \\ + Y'_{\delta\delta u} \Delta \delta(k) \Delta u(k) U(k) \\ + Y'_{vu} \Delta v(k) u(k) + Y'_{ru} \Delta r(k) \Delta u(k) L \\ + Y'_{\delta uu} \Delta \delta(k) \Delta u^2(k) \\ N'_0 U^2(k) + N'_{0u} \Delta u(k) U(k) + N'_{0uu} \Delta u^2(k) + N'_{v} \Delta v(k) U(k) \\ + N'_r \Delta r(k) U(k) L + N'_\delta \Delta \delta(k) U^2(k) \\ + \frac{N'_{vvv} \Delta v^3(k)}{U(k)} + N'_{\delta\delta\delta} \Delta \delta^3(k) U^2(k) + \frac{N'_{vvr} \Delta v^2(k) \Delta r(k) L}{U(k)} \\ + N'_{vv\delta} \Delta v^2(k) \Delta \delta(k) + N'_{v\delta\delta} \Delta v(k) \Delta \delta^2(k) U(k) \\ + N'_{\delta\delta u} \Delta \delta(k) \Delta u(k) U(k) + N'_{vu} \Delta v(k) \Delta u(k) \\ + N'_{ru} \Delta r(k) \Delta u(k) L + N'_{\delta uu} \Delta \delta^2(k) \Delta u^2(k) \end{array} \right] \quad (29)$$

According to Eq. (27), Eq. (28) and Eq. (29), the input samples and output samples can be achieved as:

Input

Table 4
The Comparison of MSE among these methods in testing trajectory.

		CS-LSSVM	PSO-LSSVM	CV-LSSVM	BPNN
Surge velocity	MSE	0.0073	0.0081	0.0086	0.0121
	TIME	42s	51s	61s	83s
Sway velocity	MSE	0.0043	0.0051	0.0058	0.0093
	TIME	38s	39s	43s	51s
Yaw rate	MSE	0.0055	0.0059	0.0059	0.0084
	TIME	44s	51s	49s	58s

Output

$$\begin{cases} \Delta u(k+1) = AX \\ \Delta v(k+1) = BY \\ \Delta r(k+1) = CZ \end{cases} \quad (34)$$

By training the input data and output data, the A , B and C are obtained. Then the hydrodynamic derivatives can be achieved at the same time. It can be calculated by the following equation:

$$\begin{bmatrix} \frac{h}{L(m' - X'_{\dot{u}})} & 0 & 0 \\ 0 & \frac{h(I'_z - N'_{\dot{r}})}{TL} & -\frac{h(m'x'_G - Y'_{\dot{r}})}{TL} \\ 0 & -\frac{h(m'x'_G - N'_{\dot{v}})}{TL^2} & \frac{h(m' - Y'_{\dot{v}})}{TL^2} \end{bmatrix} \begin{bmatrix} X'_{\dot{u}} \\ Y'_0 \\ N'_0 \end{bmatrix} = \begin{bmatrix} a_1 \\ b_1 \\ c_1 \end{bmatrix} \quad (35)$$

where h denotes time interval, L the length of USV. The other hydrodynamic derivatives can be obtained by the same way. Therefore, the set of A , B and C are important to identify the unmanned surface vehicle's dynamic.

4. Identification results

4.1. Data processing

In this section, the USV's experiment is carried out in the Qinghuai river. In Fig. 4, the left part of the draw is the real surroundings which is detected by the DW-uboats while the right is that the direction of

$$X = \left[\Delta u(k), \Delta u(k) U(k), \Delta u^2(k), \frac{\Delta u^3(k)}{U(k)}, \Delta v^2(k), \Delta r^2(k), \Delta \delta^2(k) U^2(k), \Delta \delta^2(k) \Delta u(k) U(k), \Delta v(k) \Delta r(k), \Delta v(k) \Delta \delta(k) U(k), \Delta v(k) \Delta \delta(k) U(k) \right]_{11 \times 1}^T \quad (30)$$

$$Y = \left[\Delta v(k), U^2(k), \Delta u(k) U(k), \Delta u^2(k), \Delta v(k) U(k), \Delta r(k) U(k), \Delta \delta(k) U^2(k), \frac{\Delta v^3(k)}{U(k)}, \Delta \delta^3(k) \Delta U^2(k), \frac{\Delta v^2(k) \Delta r(k)}{U(k)}, \Delta v^2(k) \Delta \delta(k), \Delta v(k) \Delta \delta^2(k) U(k), \Delta \delta(k) \Delta u(k) U(k), \Delta v(k) \Delta U(k), \Delta r(k) \Delta u(k), \Delta \delta(k) \Delta u^2(k) \right]_{16 \times 1}^T \quad (31)$$

$$Z = \left[\Delta r(k), U^2(k), \Delta u(k) U(k), \Delta u^2(k), \Delta v(k) U(k), \Delta r(k) U(k), \Delta \delta(k) U^2(k), \frac{\Delta v^3(k)}{U(k)}, \Delta \delta^3(k) U^2(k), \frac{\Delta v^2(k) \Delta r(k)}{U(k)}, \Delta v^2(k) \Delta \delta(k), \Delta v(k) \Delta \delta^2(k) U(k), \Delta \delta(k) \Delta u(k) U(k), \Delta v(k) \Delta u(k), \Delta r(k) \Delta u(k), \Delta \delta(k) \Delta u^2(k) \right]_{16 \times 1}^T \quad (32)$$

Let

$$\begin{cases} A = [1, a_1, a_2, \dots, a_{10}]_{1 \times 11} \\ B = [1, b_1, b_2, \dots, b_{15}]_{1 \times 16} \\ C = [1, c_1, c_2, \dots, c_{15}]_{1 \times 16} \end{cases} \quad (33)$$

Qinghuai river is about 45° from north-east. It is obvious that the wave and current exist in the river which means the data includes a lot of noises. Therefore, the Gaussian filtering method is utilized to move the much noise. The data collected by the receiver per 0.25 s and the 1000 s' data is adopted to obtain the dynamic model of the USV. The zigzag test of USV is designed and the red line represents the trajectory of USV. Two different parts of trajectory are selected for training and testing.

Fig. 5 shows the 1000 s' data for part trajectory of the USV. This picture demonstrates the regular of the surge velocity, sway velocity and yaw rate in zigzag trajectory. The upper sub-figure represents the commanded yaw and real yaw, the middle sub-figure denotes the surge velocity and sway velocity of DW-uBoat and the lower sub-figure is the yaw rate. It is clear that when the yaw angle changes from the 90°–200° and from 200° to 90°, the surge velocity, sway velocity and yaw rate will have significant changes in the whole trend. The black chain lines denote this phenomenon. In addition, although the data in **Fig. 5** has been filtered, the curves of the surge, sway and yaw rate is not smooth, since the randomness of external interference is too large, it is difficult to ensure the curves become smooth, it may be more difficult to identify the USV's dynamics.

4.2. Identification results

Based on the procedure of CS-LSSVM proposed in the section 3, the initial properties of CS sets are: p_a is 0.75 and n is 20. The best regularization parameter will be determined to SVM structure and the regularization parameter is 5.8×10^7 . According to the Eq. (30) - Eq. (35), the input data and output data can be calculated by the data from the zigzag test. Then the identified parameters are obtained by the LSSVM and which can be shown in **Table 2**.

The PSO and CV algorithm selected to optimize the LSSVM are considered in this section. In addition, back propagation neural network (BPNN) is always utilized to system identification and shows a well performance (Fang et al., 2017). Therefore, the CS-LSSVM is compared to the PSO-LSSVM, CV-LSSVM and BPNN in identification of USV's dynamics. **Fig. 6** shows the comparisons of the surge velocity, sway velocity and yaw rate, respectively, predicted by these methods in training trajectory and **Table 3** shows the related mean square error (MSE). It can be observed that these methods all can well predict the 3 DOF of USV's dynamics. However, for the prediction of surge velocity and sway velocity, it is obvious that the CS-LSSVM has a better predictive capability than other methods in the real environment and the related values of MSE can also support this phenomenon. In addition, the convergency speed of the CS-LSSVM is faster than other methods. It means that the cuckoo search method can easily find the best parameters of the support vector machine. **Fig. 7** shows the surge velocity, sway velocity and yaw rate in test trajectory. It can be viewed that CS-LSSVM, PSO-LSSVM and CV-LSSVM still enjoy good abilities of prediction while the BPNN is not able to predict accurately. **Table 4** shows that the results predicted by CS-LSSVM are more accuracy and the convergence speed is faster in any freedom. CV as trial and error method is a little time-consuming to obtain the suitable solution in this problem, but this method not get precise optimization results. The PSO can find the global optimum for SVM, but sometimes it fails to provide globally optimal solutions instead of locally optimal ones. The draws of BPNN is learning time is long and easily falls into the local minimums or overfittings. For the CS, owing to the cuckoo search based on levy flight is a random walk which is also a Markov chain whose next state/position only depends on the current state and the transition probability. However, other methods' new parameters should be generated by far-field randomization, and their positions should be far enough away from the current optimal solution, which will ensure that the system will not fall into local optimal. The CS-LSSVM has a better generalization ability and faster convergency speed.

In this paper, the system identification is offline, 4000 data were selected to train the dynamic models. It is tested that the CS-LSSVM has a better prediction ability than other mainstream methods. Therefore, for the online system identification in the future, this method can be a potential application to build up dynamic models of USV in the different environments (wind, wave and current etc.) in terms of computational time and finite samples.

5. Conclusion

In this paper, the abkowitz model is adopted to describe the USV's dynamics. The zigzag test of USV is carried out in the real environment with wind, current and other disturbances. For the first time, the SVM method enhanced CS algorithm is firstly proposed to identify the DW-uboat's dynamics by utilizing the experimental data. The hydrodynamic derivatives of the abkowitz model are also obtained by the CS-LSSVM. The comparison among CS-LSSVM, PSO-LSSVM, CV-LSSVM and BPNN are considered in two trajectories (one for training and one for testing), the results show that the CS-LSSVM method has better ability of identification than other methods which enjoy higher accuracy and faster convergence speed in the real environment. Therefore, this new method has a good generalization capability to identify the USV's dynamics in real environment.

Author contributions section

Peng-Fei Xu: supervision and revised the paper. Chen Cheng: write the paper and code, finish the main work in this paper. Hong-Xia Cheng: carry out the experiment. Ya-Lin Shen: carry out the experiment. Yan-Xu Ding: carry out the experiment.

Declaration of competing interest

The authors declare that they have no known competing financial interests or personal relationships that could have appeared to influence the work reported in this paper.

Acknowledgements

This work was supported by the Natural Science Foundation of Jiangsu Province (BK20160875), National Natural Science Foundation of China (51609078) and Marine Science and Technology Innovation Project of Jiangsu Province (HY2018-15).

References

- Aström, K.J., Källström, C., 1976. Identification of ship steering dynamics. *Automatica* 12 (1), 9–22.
- Fang, Y., Pang, M.Y., Wang, B., 2017. A course control system of unmanned surface vehicle (USV) using back-propagation neural network (BPNN) and artificial bee colony (ABC) algorithm. In: 8th International Conference on Advances in Information Technology, IAIT2016, 19–22 December Macau, China.
- Fossen, T.I., 2011. *Handbook of Marine Craft Hydrodynamics and Motion Control*. John Wiley & Sons.
- Luo, W.L., Zou, Z.J., 2009. Parametric identification of ship maneuvering models by using support vector machines. *J. Ship Res.* 53 (1), 19–30.
- Nadjemi, O., Nacer, T., Hamidat, A., Salhi, H., 2017. Optimal hybrid PV/wind energy system sizing: application of cuckoo search algorithm for Algerian dairy farms. *Renew. Sustain. Energy Rev.* 70, 1352–1365.
- Nguyen, H.D., 2008. Recursive identification of ship manoeuvring dynamics and hydrodynamics. *ANZIAM J.* 49, 717–732.
- Pan, C.Z., Lai, X.Z., Yang, S.X., Wu, M., 2013. An efficient neural network approach to tracking control of an autonomous surface vehicle with unknown dynamics. *Expert Syst. Appl.* 40, 1629–1635.
- Rajesh, G., Bhattacharyya, S., 2008. System identification for nonlinear maneuvering of large tankers using artificial neural network. *Appl. Ocean Res.* 30 (4), 256–263.
- Rakhshani, H., Dehghanian, E., Rahati, A., 2016. Hierarchy cuckoo search algorithm for parameter estimation in biological systems. *Chemometr. Intell. Lab. Syst.* 159, 97–107.
- Roodposhti, M.S., Safarrad, T., Shahabi, H., 2017. Drought sensitivity mapping using two one-class support vector machine algorithms. *Atmos. Res.* 193, 73–82.
- Shin, J., Kwak, D.J., Lee, Y., 2017. Adaptive path following control for an unmanned surface vessel using an identified dynamic model. *IEEE ASME Trans. Mechatron.* 22 (3), 1143–1153.
- Sketne, R., Smogeli, O., Fossen, T.I., 2004. Modeling, identification, and adaptive maneuvering of cybership: a complete design with experiments, proc. In: IFAC Conf. On Control Applications in Marine System, pp. 203–208.
- Sonnenburg, C.R., Woolsey, C.A., 2013. Modeling, identification, and control of an unmanned surface vehicle. *J. Field Robot.* 30 (3), 371–398.
- Suykens, J.A., Vandewalle, J., 1999. Least squares support vector machine classifiers. *Neural Process. Lett.* 9 (3), 293–300.
- Vapnik, V.N., 2000. *The Nature of Statistical Learning Theory*. Springer, New York.

- Walton, S., Hassan, O., Margan, K., 2013. Modified cuckoo search: a new gradient free optimization algorithm. *Chaos, Solit. Fractals* 44 (9), 710–718.
- Wang, S.T., Yuan, Y.Y., Zhu, C.Y., Kong, D.M., Wang, Y.T., 2019. Discrimination of polycyclic aromatic hydrocarbons based on fluorescence spectrometry coupled with CS-SVM. *Measurement* 139, 475–481.
- Wei, H.L., Chu, J.C., Huang, H., 2015. Study on the propulsion of the rotatable Twin-propeller propulsion ship based Equivalent Rudder angle. *J. Wuhan Univ. Technol.* 39 (3), 611–615.
- Xu, F., Zou, Z.J., Yin, J.C., Cao, J., 2013. Identification modeling of underwater vehicle's nonlinear dynamics based on support vector machines. *Ocean Eng.* 67, 68–76.
- Xu, F., Xiao, T., Xing, X., Liu, Z., 2014. Identification of Nomoto models with integral sample structure for identification. In: 2014 33rd Chinese Control Conference (CCC). IEEE, pp. 6721–6725.
- Yoon, H.K., Rhee, K.P., 2003. Identification of hydrodynamic coefficients in ship maneuvering equations of motion by estimation-before-modeling technique. *Ocean Eng.* 30 (18), 2379–2404.
- Zhang, X.G., Zou, Z.J., 2011. Identification of abkowitz model for ship manoeuvring motion using ϵ -support vector regression. *J. Hydron.* 23 (3), 353–360.
- Zhu, M., Hahn, A., Wen, Y.Q., Bolles, A., 2017. Identification-based simplified model of large container ships using support vector machines and artificial bee colony algorithm, 68, 249–261.
- Zwierzewicz, Z., 2013. On the ship course-keeping control system design by using robust feedback linearization. *Pol. Marit. Res.* 20 (1), 70–76.